



A quantum chemical investigation of the oxidation and dissolution mechanisms of Galena

ANDREA R. GERSON* and ANTHONY R. O'DEA

Ian Wark Research Institute (The Commonwealth ARC Special Research Center in Particle and Material Interfaces), University of South Australia, Mawson Lakes Campus, South Australia 5095, Australia.

(Received February 4, 2002; accepted in revised form August 20, 2002)

Abstract—The oxidation and dissolution mechanisms of galena (PbS) remain uncertain with a wide variety of possible mechanisms having been proposed in the literature. In this study, the thermodynamic viability of some possible mechanisms has been tested using semi-empirical quantum chemical calculations applied to a perfect (001) galena surface.

The adsorption of O₂ and H₂O has been examined in both the gaseous and aqueous environments. In agreement with previous *ab initio* quantum chemical calculations, the surface induced dissociation of H₂O in either environment was found to be energetically unfavourable. However, the dissociative adsorption of O₂ was found to be possible and resulted in two O atoms bonded to diagonally adjacent S atoms with the O atoms oriented along the diagonal.

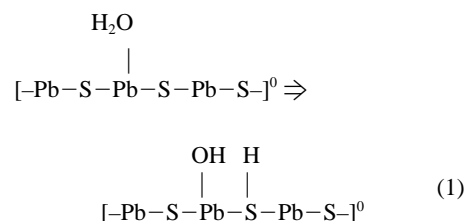
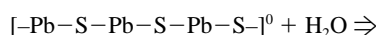
The adsorption of H⁺ and possible subsequent dissolution mechanisms have been examined in the aqueous environment. An anaerobic mechanism leading to the dissolution of hydroxylated Pb²⁺ was identified. The mechanism involves the protonation of 3 surface S atoms surrounding a central surface Pb atom followed by substitution of this Pb by a further H⁺. The activation energy of this mechanism was estimated to be ≈100 kJ mol⁻¹. Pb²⁺ dissolution could only occur with vacancy stabilisation by a H⁺. The analogous mechanisms for systems comprising H⁺ adsorbed on either 2 or 4 of the S atoms surrounding a central surface Pb were not found to be energetically viable. Subsequent dissolution of one of the protonated S atoms to form H₂S_(g) was not found to be possible thus indicating the likely formation of a Pb-deficient S-rich surface under acidic anaerobic conditions.

Acidic aerobic dissolution has also been examined. Congruent dissolution to form H₂SO₄ and Pb²⁺•6H₂O is energetically viable. The dissolution of one of the protonated S atoms neighbouring the Pb²⁺ vacancy, resulting from the anaerobic dissolution, to form H₂SO₄, is also possible. Copyright © 2003 Elsevier Science Ltd

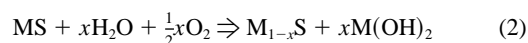
1. INTRODUCTION

The surface species found on galena on oxidation and dissolution have been studied using many techniques including scanning tunneling microscopy (Laajalehto et al., 1993; Kim et al., 1994; Kim et al., 1995), X-ray photoelectron spectroscopy (Laajalehto et al., 1991; 1993; Fornasiero et al., 1994a), fourier transform infrared spectroscopy (Laajalehto et al., 1991; Prestidge et al., 1993) and zeta potential (Fornasiero et al., 1994b). The quantum chemical calculations described herein deal solely with the first atomic-scale steps of oxidation in gaseous and aqueous environments, and dissolution in aqueous environments under acidic conditions in the presence and absence of O₂. The discussion given below, therefore, does not seek to deal with the precipitation of inhibiting layers of PbSO₄ or PbO nor the formation of polysulfides or elemental sulfur, all of which would only occur after considerable oxidation/dissolution reactions.

Surface complexation models have been used to describe adsorption at hydrous metal oxide surfaces and have explained the formation of surface hydroxyl groups (Westall, 1986). It has been assumed that similar complexation takes place at the surface of hydrous metal sulfides such as galena (Sun et al., 1991) resulting in the following hydration mechanism:



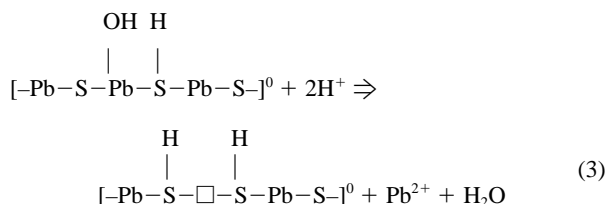
On exposure to air and aqueous solution, hydroxides form on sulfide mineral surfaces (Prestidge et al., 1994), often with a metal deficient sulfide beneath the hydroxides (Smart, 1991):



where M represents any metal. On oxidation of galena in air, a metal deficient sulfide is formed within one day, covered with a layer of lead hydroxide, oxide and carbonate (Buckley and Woods, 1984). On further exposure to air, basic sulfate and lead sulfate are also observed.

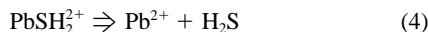
An ion exchange process between protons and metal ions is assumed to occur at the surface (Sun et al., 1991) resulting in the formation of a metal deficient surface (a □ indicates an atomic absence).

* Author to whom correspondence should be addressed (Andrea.Gerson@unisa.edu.au).

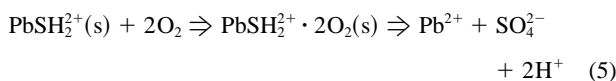


A similar reaction has been proposed (Eadington and Prosser, 1969) whereby adsorbed O and water react with the galena surface to give rise to the same galena surface structure as indicated in Eqn. 3. Sulfate only appeared after long periods (5 h) of oxidation at all pH values (Eadington and Prosser, 1969). An anodic oxidation study of galena at pH 1 also reports a metal deficient surface (Gardner and Woods, 1979).

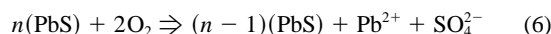
Hsieh and Huang found that the rate of Pb dissolution decreased rapidly on increasing pH (almost zero above pH 8; Hsieh and Huang, 1989). It was proposed that as the dissolution rate is much higher under acidic conditions as compared to alkaline conditions a protonated surface, PbSH_2^{2+} , initiates the dissolution process. In the absence of oxygen the following mechanism was proposed:



and in the presence of O_2



Under both O_2 and N_2 purging, a 1:1 dissolution of Pb and S was found with HS^- comprising the major S solution species with N_2 purging and SO_4^{2-} comprising the major solution S species with O_2 purging. The dissolution process in alkaline solution has been shown to be congruent but extremely slow (Hsieh and Huang, 1989). Equal concentrations of lead and sulfur species are dissolved:



Purging with O_2 as opposed to N_2 had only a minor rate enhancing effect on the concentration of Pb detected in solution (Hsieh and Huang, 1989) over a wide range of pH values. Fornasiero et al. (1994a) carried out both solution and surface analysis on oxidised/dissolved galena samples prepared at pH values of 5, 7 and 9 for 2 h. As for the study carried out by Hsieh and Huang (1989), they found that dissolution carried out under N_2 purging was slightly slower than under O_2 purging. However, dissolution using air purging was found to be the most rapid (Fornasiero et al., 1994a). Lead sulfate may react with carbon dioxide to form lead carbonate (Hagihara, 1952). Fornasiero et al. (1994a, 1994b) find lead hydroxide and oxide at high pH in the presence of N_2 (i.e., the absence of CO_2), and lead carbonate and hydroxy carbonate in the presence of air. Lead sulfate and thiosulphate are also formed in neutral to alkaline solutions in contact with air or with O_2 purging (Plant and Sutherland, 1949; Sutherland and Wark, 1955; Wells et al., 1972; Zingg and Hercules, 1978; Gardner and Woods, 1979; Buckley and Woods, 1984; Pugh and Bergstrom, 1986).

The purpose of the research reported herein is to examine the relative thermodynamics of some of the oxidation and dissolution reactions postulated to occur at galena surfaces. We have

employed a semi-empirical quantum chemical molecular modeling technique to differentiate between the likelihood of different reactions. None of the dissolution mechanisms proposed, that we are aware of, have involved the adsorption of OH^- therefore we have limited this study to the adsorption of H_2O , H^+ and O_2 .

2. MATERIAL AND METHODS

The Parametric Method 3 (PM3) (Stewart, 1989; 1991) as implemented in AMPAC (AMPAC, 1994) has been used in conjunction with COSMO—Conductor-like Screening Model (Klamt and Schürman, 1993) to model solvent effects.

PM3 is based on Neglect of Diatomic Differential Overlap (NDDO) (Pople et al., 1965). This is a self-consistent field method, taking into account both electrostatic repulsion and exchange stabilisation, i.e., stabilisation of excited states with electrons of the same spin, and all calculated integrals are evaluated by approximate means. This method uses a restricted basis set of one *s* orbital and three *p* orbitals (p_x , p_y , and p_z) per atom and ignores overlap integrals in the secular equation, i.e., the basis is assumed to be orthogonal.

The heat of formation (ΔH_f°) calculated is defined as the sum of the electronic (E_{elec}) and nuclear-nuclear repulsion (E_{nuc}) energies of the system, the total energies of the isolated atoms in the system (E_{isol}), and the heats of formation of all the atoms in the system with respect to their thermodynamic reference states (E_{atom}):

$$\Delta H_f^\circ = E_{\text{elec}} + E_{\text{nuc}} + \sum_A E_{\text{isol}}(\text{A}) + \sum_A E_{\text{atom}}(\text{A}) \quad (7)$$

Both E_{isol} and E_{atom} depend only on the type of atom, i.e., they do not depend on interactions between atoms or the geometry of the system. Since semi-empirical methods are parameterised using reference data which are conventionally given at 298 K, these methods produce ΔH_f° at this temperature.

The heat of reaction, ΔH_r° , can be calculated from the heats of formation of the reactants (A and B) in isolation from each other, and the heats of formation of the final configuration of the products (A + B):

$$\Delta H_r^\circ = \Delta H_f^\circ(\text{A} + \text{B}) - [\Delta H_f^\circ(\text{A}) + \Delta H_f^\circ(\text{B})] \quad (8)$$

A negative heat of reaction is considered indicative of a favourable reaction. Entropic effects have not been considered, as it is simply not computationally possible to do so. However, it should be remembered that it is possible for entropic contributions to affect the outcome of a reaction to the extent that a reaction may proceed even if ΔH_r° indicates otherwise. For instance dissolution may occur, due to entropic contributions, even if unfavourable in terms of enthalpy, as long as the resulting ionic activity product is small. Additionally, the calculations of ΔH_r° do not indicate the kinetics of a reaction and hence provide no information as to whether a reaction will proceed rapidly or slowly. All ΔH_r° or ΔH_f° with a further subscript _G refer to calculations carried out in the gas phase. A subscript _L refers to calculations carried out in the aqueous phase.

Bond strengths are calculated from the density matrix generated by PM3. A bond strength of 1 indicates there are 2 electrons in the bond; a bond is considered to exist if the bond strength is greater than 0.2.

2.1. Cluster Size Validation

Calculations were performed to determine the most appropriate representation of the galena surface. As the reactions to be investigated involved only small adsorbing molecules, the surface area of the PbS cluster did not have to be very large. However, it was necessary for the surface to be sufficiently large to exclude edge effects (i.e., erroneous results due to the atoms at the edge of the cluster). A point charge cluster embedding technique has been applied to Hartree Fock studies of the surface structure of galena. Surface distortion resulting from cluster termination is largely removed using this methodology and the model enables solid state properties (e.g., scanning tunneling microscopy images, scanning tunneling spectroscopy and lattice geometries)

Table 1.

ΔH_f° (kJ mol ⁻¹) for				
Reaction 1: [-Pb-S-Pb-S-Pb-S-] ⁰ → [-Pb-S-□-S-Pb-S-] ²⁺ + Pb ²⁺				
Reaction 2: [-Pb-S-Pb-S-Pb-S-] ⁰ → [-Pb-S-Pb-□-Pb-S-] ²⁺ + S ²⁻				
Reaction 3: [-Pb-S-Pb-S-Pb-S-] ⁰ + H ⁺ → [-Pb-S- $\overset{\text{H}}{\text{Pb}}$ -S-Pb-S-] ¹⁺				
Reaction 4: [-Pb-S-Pb-S-Pb-S-] ⁰ + H ⁺ → [-Pb-S-Pb- $\overset{\text{H}}{\text{S}}$ -Pb-S-] ¹⁺				
Cluster size	6 × 6 × 3	6 × 6 × 4	8 × 8 × 3	
Reaction 1: removal of Pb ²⁺	+1678	+1656		
Reaction 2: removal of S ²⁻	+1979	+1994		
Reaction 3: addition of H ⁺ onto surface Pb	-681			-688
Reaction 4: addition of H ⁺ onto surface S	-938			-942

to be well described (Becker et al., 1997; Becker and Rosso, 2001). This methodology may be applied in further studies.

A three-layer cluster, with each layer consisting of 36 atoms (stoichiometry is Pb₅₄S₅₄), where the top two layers are optimized, has been chosen as being appropriate. This cluster gives rise to a ΔH_f° per PbS group of -108 kJ mol⁻¹ which is acceptable compared to the experimental value of -98 kJ mol⁻¹ (Chase et al., 1985). The surface area of the top of the PbS cluster is approximately 220 Å² (with an interlayer spacing of 2.9681 Å) although the effective surface area (to avoid edge effects) is approximately 140 Å². An ab initio quantum chemical cluster method was not chosen due to the size of the model required. Additionally, an ab initio quantum chemical periodic 2-D surface methodology is not viable in that the 2-dimensional unit cells would have to be very large to minimise defect interaction on the model surface, and hence the computational requirements would also be very high.

The ΔH_f° calculated for the unoptimised 6×6×3 slab, the slab with 1 layer optimised, 2 layers optimised and 3 layers optimised was -5092 kJ mol⁻¹, -5587 kJ mol⁻¹, -5862 kJ mol⁻¹ and -6249 kJ mol⁻¹ respectively. Relaxation of 2 or 3 layers gave rise to the same gain in stability relative to the number of atoms optimised (i.e., $(\Delta H_f^\circ_{\text{opt}} - \Delta H_f^\circ_{\text{unopt}})/N$ where N equals the number of atoms optimised = -10.7 kJ mol⁻¹ atom⁻¹). The optimisation of 1 layer gave rise to a gain in stability of -13.7 kJ mol⁻¹ atom⁻¹. However, the use of models where only the top layer was optimised was not considered feasible for the type of mechanistic study undertaken. Formation of vacancy sites, migration of surface atoms and adsorption of surface species are all likely to affect the electronic structure and hence spatial distribution of the second atomic layer. For these reasons, we investigated further the validity of carrying out calculations using a three-layer slab with optimisation of the top two layers.

Refinement of the top two layers, with the bottom layer fixed results in a relaxation of -0.10 Å (3.2% of one monolayer) for the top layer and -0.11 Å (3.6% of one monolayer) for the second layer. Rumpling of 0.10 Å between Pb (which moves outwards) and S atoms occurs at the surface. The change in unit cell dimensions in the x and y directions on optimisation of the two layers was extremely small and less than 10⁻⁵ Å in magnitude (calculated taking into account only atomic spacings in the top two layers). Becker and Hochella (1996) using the periodic ab initio technique, Crystal92, calculate a relaxation of -0.07 Å and a rumpling of 0.10 Å (with the Pb atoms moving outwards). The quantum-chemical semi-empirical results calculated here compare well.

To test the appropriateness of the slab dimensions we have carried out some limited calculations employing slabs of different sizes. These calculations examined the removal of S²⁻ and Pb²⁺ from a slab of 6×6×4 atoms, i.e., 4 layers thick, and the addition of H⁺ to surface Pb and S atoms on a slab of 8×8×3 atoms. The ΔH_f° for these reactions is given in Table 1. The addition of a further layer of atoms, as compared to the 6×6×3 clusters results in a reduction of 22 kJ mol⁻¹ to ΔH_f° in the case of removal of Pb²⁺ and an increase of 15 kJ mol⁻¹ in the case of removal of S²⁻. There is even less variation in the ΔH_f°

for the adsorption of H⁺ onto the 8×8×3 cluster as compared to the 6×6×3 cluster; 7 kJ mol⁻¹ less in the case of H⁺ addition to surface Pb and 4 kJ mol⁻¹ less in the case of H⁺ addition to surface S. It is apparent from these calculations that the 6×6×3 cluster is an appropriate base from which to explore dissolution mechanisms of galena. Neither an increase in surface area nor thickness cause significant deviation in terms of atom addition or hole formation respectively.

2.2. Validation of the Cosmo Methodology

COSMO belongs to the class of dielectric continuum models. In these models, the solute molecule is embedded in a dielectric continuum of permittivity ϵ , i.e., the solute molecule forms a cavity within the dielectric. From electrostatic theory (Jackson, 1975), it is known that the response of a homogeneous dielectric continuum to any charge distribution of solute consists of a surface charge distribution on the interface, arising from polarisation of the dielectric medium. This is not uniform over the interface, varying with specific interactions with the solute thus mimicking variable solvent orientations. It is a non-trivial problem to calculate the screening charge densities $\sigma(\mathbf{r})$ given by

$$4\pi\epsilon\sigma(\mathbf{r}) = (\epsilon - 1)\mathbf{n}(\mathbf{r})E^-(\mathbf{r}) \quad (9)$$

where $\mathbf{n}(\mathbf{r})$ is the surface normal vector at the point \mathbf{r} , and $E^-(\mathbf{r})$ is the electric field at the inner side of the cavity surface. This cannot, in general, be solved analytically for arbitrarily shaped surfaces. Numerical approaches involve the segmentation of the cavity surface with a constant charge density σ_v on each segment S_v .

The construction of segmentation of the solvent cavity is carried out via four steps (Klamt and Schuurman, 1993). Initially a grid is projected onto the set of spheres defined by the sum of the van der Waals radii of the atoms making up the model and the effective radius of the solvent molecule. Points lying within the radii of any of the model atoms are excluded leaving only the possible positions for the centers of the solvent molecules. The points left are contracted to the minimum distance the edge of a solvent molecule may be away from the solute model. These points then represent the solvent accessible surface. In the third step these points are grouped into segments, the number of which is an input variable (m). In the fourth step, the area of each segment is calculated, as is the representation vector ($\mathbf{n}(\mathbf{r})$) describing the center of each set of points making up each segment. The screening charge distribution is then represented by a m -dimensional vector σ . Although COSMO has been applied numerous times to small molecular systems, as far as the authors are aware, this is the first time this technique has been applied to the study of solid surfaces. However, as far as the authors can ascertain there is no mathematical reason why this methodology cannot be applied to solid surfaces.

The electronic effects of the solvent are included by using COSMO, but chemical interactions of aqueous species with the surface must be examined explicitly. The heats of formation have been obtained for isolated molecules and galena slab models in a dielectric constant of $\epsilon = 18$ which was chosen to represent the dielectric constant of water within the Stern layer. This value was chosen rather than 78.6, the dielectric constant of water, based on the DLVO double-layer theory (Verwey and Overbeck, 1948). Recent calculations (Larson and Attard, 2000) used to simulate charge titration data via site binding models for titanium dioxide, aluminium oxide and silicon dioxide have found reasonable fits between experimental data and simulated data using dielectric constants of approximately 20. Hence the dielectric constant within the double layer is considerably less than that for bulk water.

To validate the use of a $\epsilon = 18$ dielectric constant for the small species employed in the reaction mechanisms, a series of calculations was carried out on (H₂O)₄ and H⁺•4H₂O using a range of dielectric constants. The most marked changes in ΔH_f° took place between $\epsilon = 0$ (i.e., ΔH_f°) and $\epsilon = 10$ with a change of -41 kJ mol⁻¹ in the (H₂O)₄ system and a far more pronounced change of -228 kJ mol⁻¹ in the H⁺•4H₂O system. It is expected that a dielectric medium will have a far greater stabilising influence on charged species than neutral species. Above $\epsilon = 10$, the rate of change of ΔH_f° as a function of ϵ decreases rapidly. There are only decreases of -8 kJ mol⁻¹ and -20 kJ mol⁻¹ for the (H₂O)₄ and H⁺•4H₂O systems respectively, between $\epsilon = 10$ and $\epsilon = 18$, and only an additional decrease of -5 kJ mol⁻¹ and -20 kJ mol⁻¹ between $\epsilon = 18$ and $\epsilon = 78.6$. As $\epsilon = 18$ gave rise

Table 2. Calculated heats of formation for the species and galena slabs used in the calculations of heats of reaction. $\Delta H_{f,G}^\circ$ is the heat formation calculated in the gas phase and $\Delta H_{f,L}^\circ$ is the heat of formation calculated for the liquid phase.

Species	$\Delta H_{f,G}^\circ$ (kJ mol ⁻¹)		$\Delta H_{f,L}^\circ$ (kJ mol ⁻¹)	
	Calculated	Experimental	Calculated	Experimental
H ₂ O	-223	-242 ^a		
(H ₂ O) ₄			-1020	-1144 ^b
H ⁺	+1480	+1531 ^a		
H ⁺ •4H ₂ O			-502	-528
Pb ²⁺	2109	2361		
Pb ²⁺ • 6H ₂ O			-569	-573
H ₂ S	-4	-20 ^c	-31	-39 ^c
H ₂ SO ₄	-782	-736 ^d	-932	-909 ^e
³ O ₂	-17	0 ^f	-17	
PbS	-108 ^g	-98 ^e	-130	

^a Weast, 1980.

^b 4(-286 kJ mol⁻¹) where -286 kJ mol⁻¹ is the experimental $\Delta H_{f,L}^\circ$ for H₂O (Rossini et al., 1952).

^c Rossini et al., 1952.

^d Chase et al., 1985.

^e Robie et al., 1978.

^f Standard state.

^g The $\Delta H_{f,G}^\circ$ for Pb₅₄S₅₄ divided by 54.

to acceptable heats of formation for aqueous species as compared to experimental values (Table 2) and is also commensurate with DLVO theory and calculations for solid surfaces it is this value of ϵ that we have used for all aqueous reaction mechanisms.

2.3. Calculated and Experimental Heats of Formation

On examination of the calculated ΔH_f° as compared to the experimental ΔH_f° for the individual species of relevance here as well as for the galena slab, reasonable agreement is achieved. Species for which the experimental ΔH_f° are available from the literature or can be calculated from literature data are provided in Table 2.

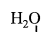
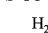
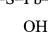
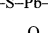
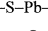
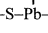
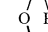
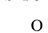
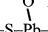
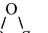
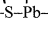
To model the behaviour of the attachment of protons to the galena surface in the aqueous phase the $\Delta H_{f,L}^\circ$ of the H⁺ has been modeled as a H⁺•4H₂O cluster. If this localised hydration is not included the sizeable instability of the lone H⁺ drives the reactions to the right in an unreasonable manner. It is the convention that the $\Delta H_{f,L}^\circ$ for H⁺ is defined as 0 kJ mol⁻¹ and that the $\Delta H_{f,L}^\circ$ for all other aqueous ionic species are defined relative to this value.

For the aqueous species H⁺•4H₂O the experimental $\Delta H_{f,L}^\circ$ can be derived from the experimental $\Delta H_{f,G}^\circ$ (H⁺) plus 4 $\Delta H_{f,G}^\circ$ (H₂O) plus $\Delta H_{r,Hyd}^\circ$ (H⁺), the heat of hydration of H⁺. $\Delta H_{f,G}^\circ$ (H⁺) is equal to +1531 kJ mol⁻¹ (Weast, 1980), $\Delta H_{f,G}^\circ$ (H₂O) is equal to -242 kJ mol⁻¹ (Chase et al., 1985) and $\Delta H_{r,Hyd}^\circ$ (H⁺) is equal to -1091 kJ mol⁻¹ (Cotton and Wilkinson, 1972) and hence the value for $\Delta H_{f,L}^\circ$ (H⁺•4H₂O) derived from the experimental values is -528 kJ mol⁻¹. This is close to the calculated value of -502 kJ mol⁻¹.

For Pb²⁺ the experimental $\Delta H_{f,G}^\circ$ is found to be +2361 kJ mol⁻¹ from the ΔH_f° of atomic Pb (+195 kJ mol⁻¹; Weast, 1980) and the sum of the ionisation potentials required to form Pb¹⁺ and Pb²⁺ sequentially (+716 and +1450 kJ mol⁻¹ respectively; Weast, 1980). The resulting value of +2361 kJ mol⁻¹ compares reasonably well, for a highly ionised species, with the calculated value of 2109 kJ mol⁻¹. It should be noted that the gas phase species Pb²⁺ does not play a role in any of the mechanisms examined.

The experimental $\Delta H_{f,L}^\circ$ for the species Pb²⁺•6H₂O can be calculated from the experimental $\Delta H_{f,G}^\circ$ for Pb²⁺ plus the sum of the $\Delta H_{f,G}^\circ$ for the H₂O and the heat of hydration, $\Delta H_{r,Hyd}^\circ$, for Pb²⁺. This latter value could not be found in the literature but can be estimated from the Born equation, literature values of $\Delta H_{r,Hyd}^\circ$ for other +2 cations and the ionic radii of these cations and Pb²⁺. The Born equation states that $\Delta H_{r,Hyd}^\circ$ is inversely proportional to the ionic radii for a constant

Table 3. Heats for formation in the gas and aqueous phase ($\Delta H_{f,G}^\circ$ and $\Delta H_{f,L}^\circ$) for the clusters formed via hydration and oxygen adsorption.

Species	$\Delta H_{f,G}^\circ$ (kJ mol ⁻¹)	$\Delta H_{f,L}^\circ$ (kJ mol ⁻¹)
[-Pb-S-Pb-S-Pb-S-] ⁰	-5862	-7030
 [-Pb-S-Pb-S-Pb-S-] ⁰	-6092	-7271
 [-Pb-S-Pb-S-Pb-S-] ⁰	-6098	-7244
 [-Pb-S-Pb-S-Pb-S-] ⁰	-5973	-7157
 [-Pb-S-Pb-S-Pb-S-] ⁰	-5734	-6917
 [-Pb-S-Pb-S-Pb-S-] ⁰	(-5581 triplet)	(-6701 triplet)
 [-Pb-S-Pb-S-Pb-S-] ⁰	-5649	-6881
 [-Pb-S-Pb-S-Pb-S-] ⁰	(-5590 triplet)	(-6627 triplet)
 [-Pb-S-Pb-S-Pb-S-] ⁰	-5727	-6888
 [-Pb-S-Pb-S-Pb-S-] ⁰	-5387	-6658
 [-Pb-S-Pb-S-Pb-S-] ⁰	-5846	-7042
 [-Pb-S-Pb-S-Pb-S-] ⁰	-5868	-7090

solvent and a constant ionic charge. Hence from known $\Delta H_{r,Hyd}^\circ$ and ionic radii (Be²⁺ -2494 kJ mol⁻¹ and 0.35 Å, Mg²⁺ -1921 kJ mol⁻¹ and 0.66 Å, Ca²⁺ -1577 kJ mol⁻¹ and 0.99 Å, Sr²⁺ -1443 kJ mol⁻¹ and 1.12 Å, Ba²⁺ -1305 kJ mol⁻¹ and 1.34 Å, Cr²⁺ -1904 kJ mol⁻¹ and 0.89 Å, Co²⁺ -1996 kJ mol⁻¹ and 0.63 Å, Zn²⁺ -2046 kJ mol⁻¹ and 0.74 Å, Mn²⁺ -1841 kJ mol⁻¹ and 0.80 Å, Ni²⁺ -2105 kJ mol⁻¹ and 0.69 Å, Cd²⁺ -1807 kJ mol⁻¹ and 0.97 Å, Fe²⁺ -1946 kJ mol⁻¹ and 0.74 Å, Cu²⁺ -2100 kJ mol⁻¹ and 0.72 Å and Hg²⁺ -1824 kJ mol⁻¹ and 1.1 Å, ionic radii from Weast, 1980) it is possible to calculate an interpolative line of best fit (of correlation coefficient 0.85) and calculate a $\Delta H_{r,Hyd}^\circ$ for Pb²⁺, ionic radius 1.2 Å of -1482 kJ mol⁻¹. Thus the $\Delta H_{f,L}^\circ$ for Pb²⁺•6H₂O derived from experimental data is calculated to be -573 kJ mol⁻¹. This is very close to our calculated value of -569 kJ mol⁻¹.

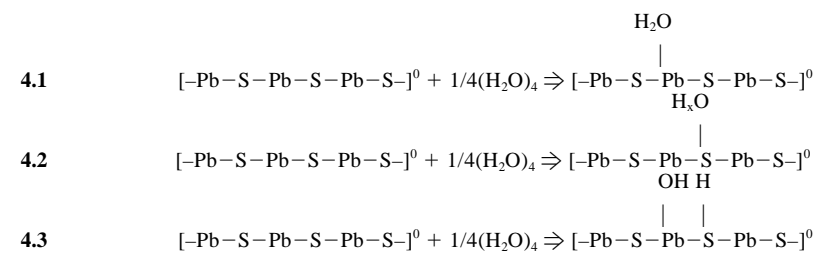
3. RESULTS AND DISCUSSION

3.1. Hydration

The adsorption and dissociation of water at the surface of galena has been examined quantum-chemically. These calculations have been carried out in both the gas and aqueous phase as they are of interest in terms of both oxidation in air and oxidation and dissolution in the aqueous environment. Initially an H₂O molecule was placed horizontally 2 Å above the surface with the O atom centered over either a Pb or S surface atom before optimisation. The relevant $\Delta H_{f,G}^\circ$ and $\Delta H_{f,L}^\circ$ for all the slab structures involved in the reaction mechanisms described in this section can be found in Table 3.

Attachment of a water molecule to a surface lead atom is slightly unfavourable in both the gas phase and aqueous phase ($\Delta H_{f,G}^\circ = +13$ kJ mol⁻¹, $\Delta H_{f,L}^\circ = +14$ kJ mol⁻¹, Eqn. 4.1, Table 4). Taking into account the likely magnitude of error inherent in these calculations it is possible the interaction of

Table 4. Hydration reactions examined in Section 3.1. The numbers in the first column are the reaction numbers referred to in the text.



H₂O with surface Pb atoms may be favourable. The O atom to Pb distance increased from 2.0 Å, the initial Pb to O distance, to 2.9 Å in both the gaseous and aqueous environments. The interaction which is responsible for the O to Pb distance equilibrating at 2.9 Å is electrostatic in origin and is of the order of -9 kJ mol^{-1} ($\Delta H_{f,G}^{\circ}(\text{cluster} + \text{H}_2\text{O}) - (\Delta H_{f,G}^{\circ}(\text{H}_2\text{O}) + \Delta H_{f,G}^{\circ}(\text{cluster}))$ where the isolated H₂O and cluster are of the geometry optimised for the cluster + H₂O system). Attachment of a water molecule to a surface sulfur atom is predicted to be unfavourable in the aqueous phase and is uncertain in the gas phase ($\Delta H_{f,G}^{\circ} = +7 \text{ kJ mol}^{-1}$, $\Delta H_{f,L}^{\circ} = +41 \text{ kJ mol}^{-1}$, Eqn. 4.2, Table 4). The final S to H distance (the shortest distance of interaction) is over 3.5 Å in both the gaseous and aqueous environments indicating little interaction is taking place between the water molecule and the surface.

The heat of reaction for the complete dissociative adsorption of H₂O is unfavourable in both the gas and aqueous phases ($\Delta H_{f,G}^{\circ} = +132 \text{ kJ mol}^{-1}$, $\Delta H_{f,L}^{\circ} = +128 \text{ kJ mol}^{-1}$, Eqn. 4.3, Table 4) even though in both cases strong bonds are formed between HO-Pb and H-S (bond strength both 0.9 in the gas phase and 0.7 and 0.9 respectively in the aqueous phase). These results indicate that dissociative adsorption of water will not occur on perfect (100) galena surfaces. This conclusion is supported by calculations performed on cluster models at both semi-empirical and ab initio levels (Wright et al., 1999) that demonstrated that H₂O would not dissociate on a perfect (001) face. These results indicate the mechanism as shown in Eqn. 1 will not occur on a perfect (001) galena surface and hence the subsequent dissolution mechanism as shown in Eqn. 3 (Sun et al., 1991) will also not occur.

3.2. Anaerobic Dissolution

The calculations described in this Section involve the surface adsorption of charged species and/or complete removal of surface species and therefore have been calculated only in the aqueous environment. In all cases the H⁺ were initially placed 1 Å above either surface Pb or S atoms. $\Delta H_{f,L}^{\circ}$ for the resulting slab structures are given in Table 5.

The direct removal of a surface Pb²⁺ to form Pb²⁺•6H₂O in a neutral aerobic environment, leaving a -2 charged surface is not energetically favourable ($\Delta H_{f,L}^{\circ} = +491 \text{ kJ mol}^{-1}$, Eqn. 6.1, Table 6). Additionally the release of PbOH⁺ into solution will not occur as the dissociation of H₂O has been shown to be unfavourable. S²⁻ dissolution in the absence of H⁺, O₂ or H₂O dissociation is unlikely (and has not been proposed in the literature) as neither protonated S species nor sulfate can result.

Hence the emphasis within this section is on mechanisms involving the adsorption of H⁺.

Protonation of a surface Pb atom has been examined in the aqueous phase and was found to be unfavourable ($\Delta H_{f,L}^{\circ} = +183 \text{ kJ mol}^{-1}$, Eqn. 6.2, Table 6) whereas aqueous protonation of a surface sulfur atom is favourable ($\Delta H_{f,L}^{\circ} = -82 \text{ kJ mol}^{-1}$, Eqn. 6.3, Table 6). Further discussion will focus on reactions subsequent to S protonation only. The disruption to bonding on H⁺ adsorption onto a surface S atom is relatively minor with only the bond from the surface S to the second layer Pb being broken (the bond strength is reduced from 0.4 to 0.1). However, the surface bonding is weakened with two bonds being reduced from 0.3 to 0.2 and the other two bonds being

Table 5. Heats of formation in aqueous phase ($\Delta H_{f,L}^{\circ}$) for the clusters formed via charged species adsorption or dissolution.

Species	$\Delta H_{f,L}^{\circ}$ (kJ mol ⁻¹)	Species	$\Delta H_{f,L}^{\circ}$ (kJ mol ⁻¹)
$[-\text{Pb}-\text{S}-\square-\text{S}-\text{Pb}-\text{S}-]^{2+}$	-7500	$[-\text{Pb}-\text{S}-\overset{\text{H}}{\text{Pb}}-\text{S}-\text{Pb}-\text{S}-]^{1+}$	-6329
$[-\text{Pb}-\text{S}-\overset{\text{H}}{\text{Pb}}-\text{S}-\text{Pb}-\text{S}-]^{1+}$	-6594	$[-\text{Pb}-\text{S}-\text{Pb}-\overset{\text{H}}{\text{S}}-\text{Pb}-\text{S}-]^{1+}$	-6441
$[-\text{Pb}-\text{S}-\overset{\text{H}}{\text{Pb}}-\overset{\text{H}}{\text{S}}-\text{Pb}-\text{S}-]^{2+}$	-5862	$[-\text{Pb}-\text{S}-\text{Pb}-\overset{\text{H}}{\text{S}}-\overset{\text{H}}{\text{S}}-\text{Pb}-\text{S}-]^{2+}$	-6019
$[-\text{Pb}-\text{S}-\overset{\text{H}}{\text{Pb}}-\overset{\text{H}}{\text{S}}-\text{Pb}-\text{S}-]^{2+}$	-6128	$[-\text{Pb}-\text{S}-\text{Pb}-\overset{\text{H}}{\text{S}}-\text{Pb}-\text{S}-]^{3+}$	-5655
$[-\text{Pb}-\text{S}-\overset{\text{H}}{\text{Pb}}-\overset{\text{H}}{\text{S}}-\overset{\text{H}}{\text{S}}-\text{Pb}-\text{S}-]^{4+}$	-5154	$[-\text{Pb}-\text{S}-\square-\text{S}-\text{Pb}-\text{S}-]^{2+}$	-6041
$[-\text{Pb}-\text{S}-\square-\text{S}-\text{Pb}-\text{S}-]^{0}$	-6893	$[-\text{Pb}-\text{S}-\overset{\text{H}}{\text{H}}-\overset{\text{H}}{\text{S}}-\text{Pb}-\text{S}-]^{1+}$	-6426
$[-\text{Pb}-\text{S}-\overset{\text{H}}{\text{H}}-\overset{\text{H}}{\text{S}}-\text{Pb}-\text{S}-]^{2+}$	-5966	$[-\text{Pb}-\text{S}-\overset{\text{H}}{\text{H}}-\overset{\text{H}}{\text{S}}-\text{Pb}-\text{S}-]^{3+}$	-5532
$[-\text{Pb}-\text{S}-\overset{\text{H}}{\text{H}}-\overset{\text{H}}{\text{S}}-\text{Pb}-\text{S}-]^{4+}$	-5028	$[-\text{Pb}-\text{S}-\overset{\text{H}}{\text{H}}-\overset{\text{H}}{\text{S}}-\square-\text{Pb}-\text{S}-]^{3+}$	-5374
$[-\text{Pb}-\text{S}-\text{Pb}-\square-\text{Pb}-\text{S}-]^{2+}$	-5955	$[-\text{Pb}-\text{S}-\square-\square-\text{Pb}-\text{S}-]^{0}$	-6746

Table 6. Anaerobic reactions examined in Section 3.2. The numbers in the first column are the reaction numbers referred to in the text.

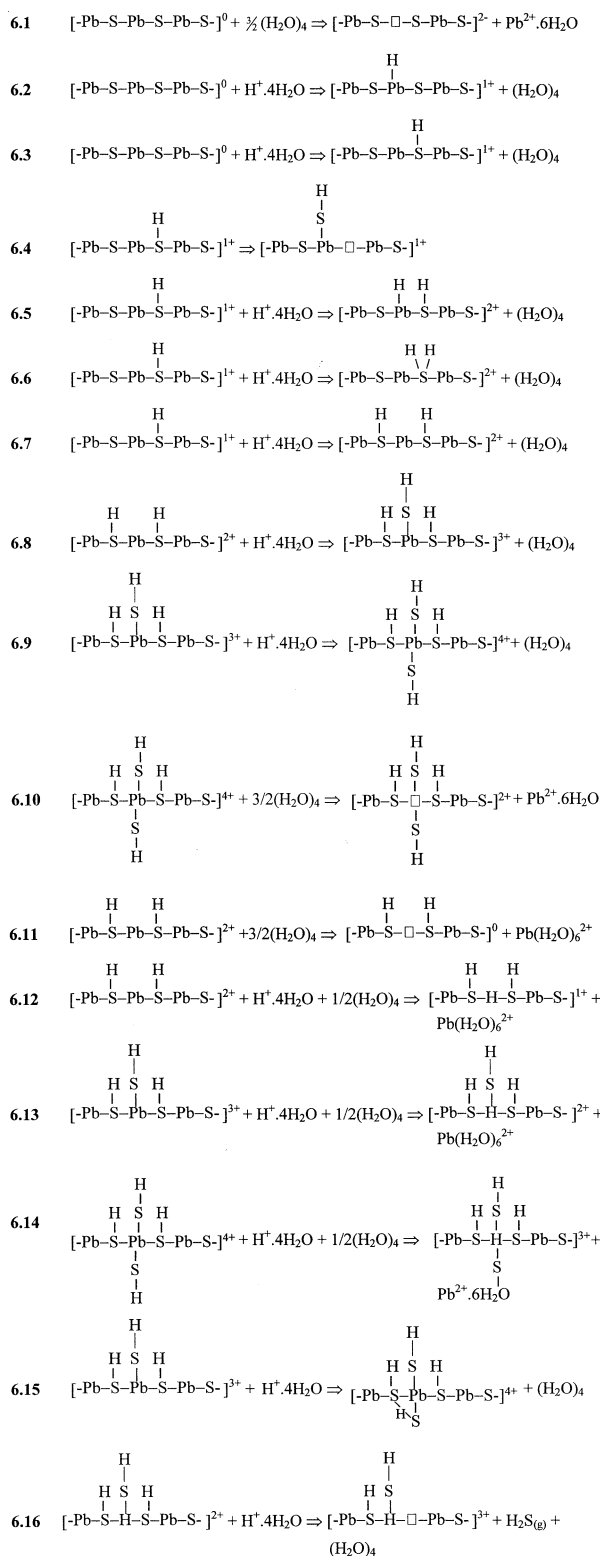
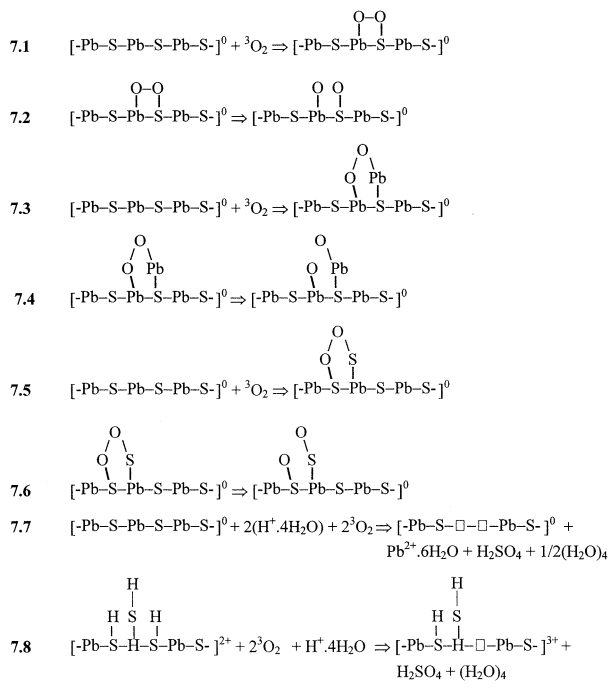


Table 7. Aerobic reactions examined in Section 3.3. The numbers in the first column are the reaction numbers referred to in the text.



reduced from 0.4 to 0.3. Even though protonation weakens the bonding of surface S atoms, migration of a protonated surface S atom proved to be unfavourable ($\Delta H_{r,L}^\circ = +153 \text{ kJ mol}^{-1}$, Eqn. 6.4, Table 6).

The attachment of a second proton onto an adjacent Pb atom is unfavourable ($\Delta H_{r,L}^\circ = +214 \text{ kJ mol}^{-1}$, Eqn. 6.5, Table 6) as is the attachment of a second proton to the same S ($\Delta H_{r,L}^\circ = +57 \text{ kJ mol}^{-1}$, Eqn. 6.6, Table 6). The double protonation of a surface S to form PbSH_2^{2+} (Hsieh and Huang, 1989) and the subsequent dissolution mechanisms (Eqn. 4 and 5) are therefore unlikely. However, the subsequent addition of a second proton onto a neighbouring S atom is favourable ($\Delta H_{r,L}^\circ = -52 \text{ kJ mol}^{-1}$, Eqn. 6.7, Table 6). The further addition of a third proton, so that three surface S atoms surround a central Pb atom is also energetically favourable ($\Delta H_{r,L}^\circ = -45 \text{ kJ mol}^{-1}$, Eqn. 6.8, Table 6) as is the addition of a fourth H^+ so that 4 H^+ surround a central surface Pb atom ($\Delta H_{r,L}^\circ = -17 \text{ kJ mol}^{-1}$, Eqn. 6.9, Table 6). The additional S atoms in the product of Eqn. 6.8 and in the reactants and products for Eqn. 6.9 (and extra S and Pb atoms which periodically also appear in subsequent reactions) represent a portion of the surface structure, which is there in all calculations, but which for simplicity is neglected where not needed in the schematic reactions depicted in the species shown in Tables 3 and 5 and Equations shown in Tables 6 and 7. It is apparent that as progressively more H^+ are added to the surface the $\Delta H_{r,L}^\circ$ for each H^+ addition becomes progressively less favourable. This is not unexpected due to the repulsion between the H^+ species on the surface of the galena. Even from a surface with 4 adsorbed H^+ , the subsequent dissolution of the central Pb^{2+} is not favourable ($\Delta H_{r,L}^\circ = +74 \text{ kJ mol}^{-1}$, Eqn. 6.10, Table 6).

The removal of a Pb atom central to two surface protonated S atoms is also unfavourable ($\Delta H_{r,L}^{\circ} = +195 \text{ kJ mol}^{-1}$, Eqn. 6.11, Table 6). Hence the product of Eqn. 3 (Sun, 1991) is unlikely to form either via H_2O dissociation or proton adsorption. However, if the Pb vacancy created is stabilised by a third H^+ (initially placed 1 \AA above the 2nd layer S) then the resulting reaction is slightly less endothermic ($\Delta H_{r,L}^{\circ} = +145 \text{ kJ mol}^{-1}$, Eqn. 6.12, Table 6) and thus the vacancy is stabilised by the presence of the additional H^+ . If a Pb^{2+} vacancy central to 3 adsorbed H^+ is stabilised by a further H^+ (bonded to the 2nd layer S), so that there are then 4 adsorbed H^+ , the removal of Pb^{2+} from the surface is favourable ($\Delta H_{r,L}^{\circ} = -34 \text{ kJ mol}^{-1}$, Eqn. 6.13, Table 6). If the Pb^{2+} central to 4 surface adsorbed H^+ is replaced by H^+ in the same manner then the reaction becomes endothermic ($\Delta H_{r,L}^{\circ} = +65 \text{ kJ mol}^{-1}$, Eqn. 6.14, Table 6) due to the high degree of localised repulsive positive charge on the galena surface.

From the calculations described above an energetically viable Pb^{2+} anaerobic dissolution mechanism in acidic media has been identified. This mechanism consists of the surface adsorption of 3 H^+ surrounding a central surface Pb atom, which is then replaced by a further H^+ . The initial unprotonated relaxed surface is shown in Figure 1a. The surface after a single protonation is shown in Figure 1b, after a second protonation in Figure 1c and after a third protonation in Figure 1d. Figures 1b, 1c and 1d correspond to the products in the aqueous phase in reactions 6.3, 6.7 and 6.8 respectively. Figure 1f shows the final structure (Eqn. 6.13) with a fourth proton filling the Pb^{2+} vacancy.

It is likely that the activation energy (E_a) associated with the dissolution of $\text{Pb}(\text{H}_2\text{O})_6^{2+}$ via the reaction shown in Eqn. 6.13 is associated with the penetration of the first layer of galena by a H^+ . To test whether the E_a is reasonable, an H^+ was placed midway between two S atoms (product of Eqn. 6.8), one S already protonated and the one S not protonated, neighbouring the Pb galena surface atom. All first and second layer atomic positions were allowed to relax except the interstitial proton (Fig. 1e). The $\Delta H_{r,L}^{\circ}$ required to form this structure was calculated to be $+109 \text{ kJ mol}^{-1}$ (Eqn. 6.15, Table 6). This is a quite reasonable E_a in the aqueous phase, thus providing further evidence of the feasibility of this mechanism for the dissolution of Pb^{2+} from galena surfaces. The interstitial proton forms strong bonds (0.4) to both of the nearest S atoms. The bonds between the S atoms bonded to the interstitial H atom, and the neighbouring Pb atoms are weakened commensurately. Relaxation of the entire system including the interstitial proton results in the interstitial proton moving slightly up out of the surface of the cluster and thus interacting significantly with only one S atom. This is not likely to be representative of a geometry that realistically represents that of the E^a structure.

The subsequent removal of a H_2S species is found to be endothermic ($\Delta H_{r,L}^{\circ} = +236 \text{ kJ mol}^{-1}$, Eqn. 6.16, Table 6). The formation of $\text{H}_2\text{S}_{(g)}$ on galena dissolution has been reported by some researchers (e.g., Fornasiero et al., 1994a). However, Higgins and Hamers (1995) concluded that the dissolution of S via the formation of H_2S occurred exclusively at step edges for pure galena with the simultaneous reduction of Pb^{2+} to Pb^0 that would then leave the galena surface uncharged. This conclusion is not in disagreement with the results

of the calculations presented in this Section, which has examined dissolution for a perfect (100) galena face.

The reaction sequence proposed here provides a possible mechanism for the dissolution of Pb^{2+} and the formation of a S-rich Pb-deficient galena surface. It is possible that this mechanism forms the first step towards the polysulfide species observed by Buckley and Woods (1984) and Kartio et al. (1996) or the elemental sulfur observed by Wittstock et al. (1996), and Kartio et al. (1998) on incongruous galena dissolution.

3.3. Aerobic Dissolution

Calculations, in both the gas and aqueous phases, have been carried out to identify how O_2 can adsorb and dissociate on the surface of galena. These calculations are of relevance to gas and aqueous phase oxidation as well as aqueous phase aerobic dissolution. A number of different geometries for both molecular adsorbed O_2 and dissociated 2O on the galena surface have been examined. The $\Delta H_{f,G}^{\circ}$ and $\Delta H_{f,L}^{\circ}$ of these species are given in Table 3.

When O_2 is initially positioned horizontally 1 \AA above the surface and equidistant between an adjacent Pb and S atom, the adsorption of the oxygen molecule is predicted to be unfavourable in both the gas and aqueous phase ($\Delta H_{f,G}^{\circ} = +145 \text{ kJ mol}^{-1}$, $\Delta H_{f,L}^{\circ} = +130 \text{ kJ mol}^{-1}$, Eqn. 7.1, Table 7). Its subsequent dissociation is also predicted to be unfavourable ($\Delta H_{f,G}^{\circ} = +104 \text{ kJ mol}^{-1}$, $\Delta H_{f,L}^{\circ} = +53 \text{ kJ mol}^{-1}$, Eqn. 7.2, Table 7). If these systems are optimised using a triplet state the resulting structures are always less stable than the singlet state. All further calculations were therefore carried out with a singlet spin state. The singlet state has also been shown by Becker and Hochella (1996) to be the most stable state for molecular O_2 when it is in close proximity to the galena surface ($<2 \text{ \AA}$).

Four further possible structures have been examined: O_2 1 \AA above the surface positioned diagonally either between two Pb or two S atoms (i.e., the surface atom to O distance is 1.79 \AA) and two O atoms placed diagonally 1 \AA directly above either two Pb or two S atoms. In the cases where O was associated with Pb either in a molecular or dissociated state the resulting structures were always less stable than the initial structures, i.e., O_2 will not adsorb in either the gas or aqueous phase and if it were to adsorb it would not dissociate (molecular O_2 : $\Delta H_{f,G}^{\circ} = +152 \text{ kJ mol}^{-1}$, $\Delta H_{f,L}^{\circ} = +159 \text{ kJ mol}^{-1}$, Eqn. 7.3, Table 7; dissociated 2O: $\Delta H_{f,G}^{\circ} = +340 \text{ kJ mol}^{-1}$, $\Delta H_{f,L}^{\circ} = +230 \text{ kJ mol}^{-1}$, Eqn. 7.4, Table 7).

In contrast, the molecular O_2 placed diagonally between 2 S atoms spontaneously disassociates. The two resulting O atoms are bonded to the diagonally opposite S atoms and are orientated towards each other with the same S-O bond lengths in both the gas and aqueous phases of 1.72 \AA . The resulting O to O distance increases from 1.23 \AA (in O_2) to 2.05 \AA . The heats of reaction for the adsorption process in the gas and aqueous phases are positive ($\Delta H_{f,G}^{\circ} = +33 \text{ kJ mol}^{-1}$, $\Delta H_{f,L}^{\circ} = +5 \text{ kJ mol}^{-1}$, Eqn. 7.5, Table 7) but only slightly so, particularly for the aqueous phase. If the system with two dissociated O atoms placed above two S atoms is optimized the O atoms align along the S to S diagonal and are oriented in the same direction. This is the same geometry as observed by Becker and Hochella

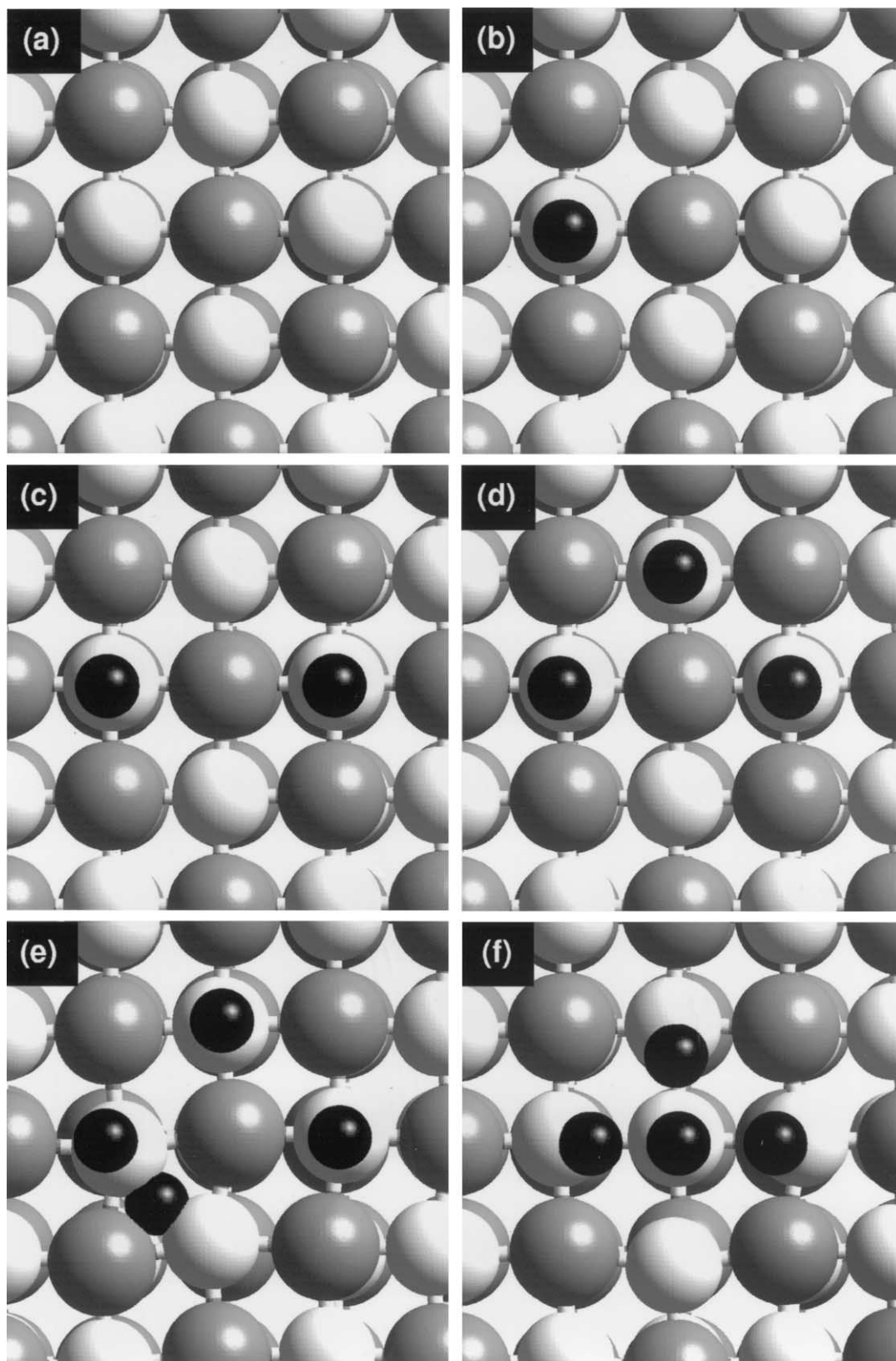


Fig. 1. The cluster models that make up the mechanism that gives rise to the metal-deficient sulfur-rich surface in an acidic aqueous environment. Pb atoms are grey, S atoms are white and H atoms are black. (a) View from above of the cluster with the top two layers of atoms refined. (b), (c) and (d) are after the addition of one, two and three H^+ respectively. (e) shows the proposed transition structure (giving rise to the E_a) where a fourth H^+ is penetrating the upper lattice layer. (f) shows the final structure in the series where the interstitial H^+ shown in (e) has pushed the central Pb atom out of the top layer of the lattice to form the aqueous species $\text{Pb}(\text{H}_2\text{O})^{6+}$.

(1996) during the process of initial surface oxidation. The rearrangement, from the system resulting from adsorbed molecular O₂, to the system resulting from the adsorption of dissociated 2O, is exothermic ($\Delta H_r^\circ G = -22 \text{ kJ mol}^{-1}$, $\Delta H_r^\circ L = -48 \text{ kJ mol}^{-1}$, Eqn. 7.6, Table 7).

If the heat of reaction for the overall O₂ adsorption process is examined, i.e., Eqn. 7.5 and 7.6 are added together, the resulting heat of reaction in the gas phase is $+11 \text{ kJ mol}^{-1}$ and in the aqueous phase -43 kJ mol^{-1} . Taking into account possible inaccuracies in these calculations the gas phase interaction of O₂ and the galena surface cannot be ruled out. Becker and Hochella (1996) further optimized the surface geometry with adsorbed O atoms and found that the dissociated O atoms may penetrate the first atomic layer of the galena and that this geometry is even more stable than that for the surface adsorbed O species. The surface oxidation calculations presented here are in very good agreement with those presented by Becker and Hochella (1996). Therefore a possible pathway for surface O₂ adsorption in both the gas and aqueous phase has been established. We have therefore justified the further exploration of aerobic acidic galena dissolution mechanisms.

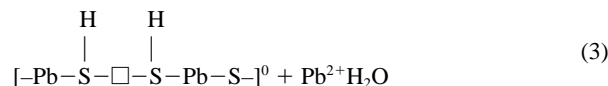
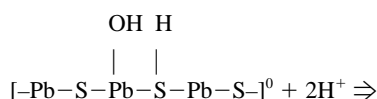
It has been shown that the rate of dissolution of galena is slightly enhanced by O₂ availability (Fornasiero et al., 1994a). In agreement with this experimental observation, the congruent dissolution of both Pb²⁺ and S²⁻ to form H₂SO₄ and Pb²⁺·6H₂O is energetically favourable ($\Delta H_r^\circ L = -689 \text{ kJ mol}^{-1}$, Eqn. 7.7, Table 7). This would provide the same products as for Eqn. 5 albeit via a different mechanism. Double protonation of a surface S atom has already been shown to be energetically unfavourable. This indicates that congruent dissolution may occur in aerobic acid conditions. (The $\Delta H_r^\circ L$ for the products from Eqn. 7.7 and 7.8 are given in Table 5).

The possibility was examined that dissolution of S²⁻ occurs as H₂SO₄ in aerobic conditions, subsequent to the dissolution of Pb²⁺ via Eqn. 5.14. This reaction was also found to be highly favourable ($\Delta H_r^\circ L = -824 \text{ kJ mol}^{-1}$, Eqn. 7.8, Table 7). Hence, congruent subsequent dissolution of S²⁻ may occur if Pb²⁺ dissolution has already occurred, via the mechanism proposed in Section 3.2.

4. CONCLUSIONS

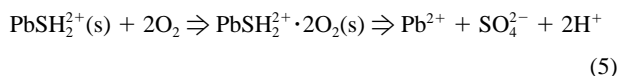
Quantum chemical calculations have been used to determine the thermodynamic likelihood of various reactions potentially involved in the oxidation and dissolution of galena from perfect (001) faces. These reactions have been compared using the heat of reaction calculated from the heats of formation of the products and reactants involved in the reaction.

Reactions relating to the adsorption and dissociation of H₂O and O₂ have been examined in both gas and aqueous environments. Neither the adsorption nor the dissociation of water on a perfect galena (001) surface is predicted to occur in either the gaseous or aqueous environment. This result is in agreement with the calculations carried out by Wright et al. (1999) and indicates the dissolution mechanism via Eqn. 3 is unlikely to occur:



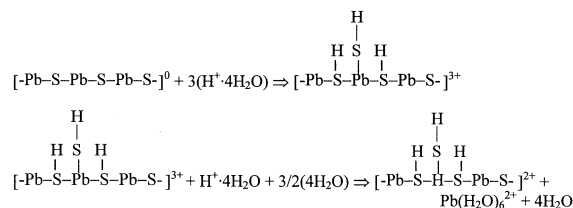
O₂ was found to adsorb dissociatively resulting in the two O atoms being bonded to two diagonally adjacent S atoms with the O atoms oriented along the diagonal. This is in agreement with calculations carried out by Becker and Hochella (1996).

The adsorption of H⁺ onto a surface S atom in the aqueous phase is found to be favourable whereas the adsorption onto a surface Pb atom is not favourable. Addition of two H⁺ onto one surface S atom was not energetically favourable thus ruling out dissolution via Eqn. 4 or 5:



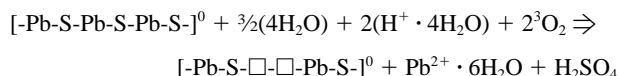
The step-wise additions of four protons onto S atoms surrounding a central Pb atom are found to be energetically favourable. The heat of reaction decreases on each subsequent addition due to the increasing repulsion between the surface H⁺ groups.

The dissolution of Pb²⁺ from various protonated surfaces was examined. The only energetically favourable acidic anaerobic dissolution mechanism identified involved the replacement of a Pb²⁺, central to three protonated S atoms, by a further H⁺:



If the activation energy for this process is assumed to be associated with the penetration of a H⁺ into the first atomic layer of the galena, a activation energy of approximately 100 kJ mol⁻¹ is calculated. Subsequent dissolution of one of the protonated S atoms as H₂S was not found to be viable, thus indicating the likely formation of a Pb-deficient S-rich surface under anaerobic acidic conditions.

Congruent dissolution in the presence of oxygen has been proposed by Hsieh and Huang (1989) and is supported by solution analysis (Fornasiero et al., 1994a) (Eqn. 5). Congruent dissolution has been shown to be energetically feasible:



In addition the protonated S atom, adjacent to the Pb²⁺ formed by aerobic dissolution, may dissolve in an acidic aerobic environment:

Acknowledgments—One of us (ARO'D) gratefully acknowledges the receipt of an AINSE (Australian Institute of Nuclear Science and Engineering) scholarship.

Associate editor: U. Becker

